Synthesis of Gold Nanoparticles Via Chemical Reduction of Au (III) Ions by Isatin in Aqueous solutions: Ligand Concentrations and pH Effects

*Ahlam Jameel Abdulghani** *Rasha K. Hussain**

Received 5, September, 2013
Accepted 26, September, 2013

Abstract:

Synthesis of gold nanoparticles (GNPs) from the reduction of tetracloroaurate(III) ($AuCl_4^-$) anions by isatin (1H-indole-2,3-dione) was achieved in aqueous solution without the use of reducing nor dispersing agents and GNPs were characterized by UV-visible absorption spectroscopy, SEM, TEM, AFM and X-ray diffraction (XRD) and FTIR analyses . The reduction process was monitored with time by measuring the UV-visible spectra of the nanoparticle solutions at different ligand concentrations and pH values. Concentrations of isatin varied from 0.034- 0.476 mM. Reduction of the Au(III) ions to form stable spherical GNPs with high extinction surface plasmon band (SPB) in range of λ 530-535 nm was found to increase with increased concentration of isatin from 0.170- 4.76 mM. The effects of pH (2.4-11.85) on the rate of synthesis, stability, morphology and particle size of GNPs were also studied spectrophotometrically. Best results were obtained at pH 5.8.

Kew words: Isatin, Surface plasmon resonance, pH, Uv-visible spectrophotometry

Introduction:

Gold nanoparticles (GNPs) have attracted increasing attention due to their unique properties in multidisciplinary applications in industry [1] photoelectronics [2,3] , catalysis [4], medicine [5], pharmacology [6], biosensor [7,8] and drug delivery [5,6,9,10]. One of the most important characteristics of the gold colloids is to create a surface plasmon band to enable their potential applications in sensors, catalysis and biosynthesis [5, 7, 11-14]. With the advancement of nanotechnology, functionalized GNPs nanoparticles have been used to conjugate different drugs [5, 6, 15]. In most of the cases amines [16,17], amino acids [18,19, 20, 21] thionine [22], gallic acid [10], glutamate [23] or linoleic acid [11] were used as functionalizing agents.

Gold nanoparticles were prepared by simple chemical reduction of tetrachloro auric acid ($HAuCl_4$) with sodium citrate [5,12, 24,25,26], sodium borohydride ($NaBH_4$) [27-31] or ascorbic acid [12, 32] in water in the presence or absence of different stabilizers [19] according to the following equation:

$$AuCl_4^- + 3e^- \rightarrow Au + 4Cl^- \quad E^o = 1.002V$$

A wide range of amino acids molecules have been used to reduce $AuCl_4^-$ forming water dispersible GNPs with different particle sizes [19, 20, 21]. Tryptophan, which is an indole essential amino acid, is among the amino acids that has been reported to reduce $AuCl_4^-$ in water in presence and absence of reducing agent [18, 19]. Isatin (1H-indole-2, 3- dione, Is) is an endogenous compound that is widely distributed in mammalian tissues and body fluids [33-36]. It is a proposed

*University of Baghdad, College of Science, Department of Chemistry, Jaderiya, Baghdad, Iraq

oxidative metabolite of tryptophan in an iron catalyzed oxidation reaction [28] (scheme 1). In nature, isatin is found in plants of the genus *Isatis* in *Calanthe* discolor LINDL [33-36]. It has also been found in humans as

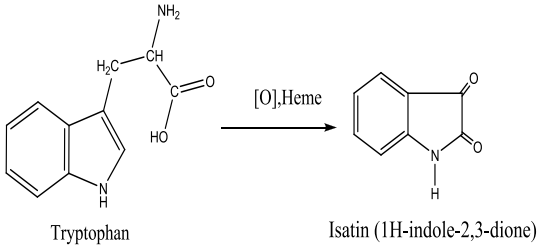

Scheme 1: Metabolic oxidation of tryptophan

a metabolic derivative of adrenalin [33,34]. Isatin and its derivatives showed a variety of biological and pharmacological activities as insecticides, fungicides, anticancer, anti-inflammatory, CNS depressant, anti-HIV, anlagesic, antianxiety and many other activities [37-43]. Due to its cis α – dicarbonyls, isatin is a potentially good substrate for synthesis of metal complexes [33, 44-46]. It has been reported that isatin was oxidized by hydrogen peroxide, chromic anhydride, or acid solutions to yield isatoic anhydride [33,47,48]. The latter is highly susceptible to hydrolysis in aqueous solutions forming anthranilic acid as a final product [33,47,48] (scheme 2). These important characteristics prompted us to investigate the capability of isatin to act as a reducing and capping agent in the synthesis of gold nanoparticles in aqueous solutions at different conditions without the addition of reducing or dispersing agents. The detection of GNPs were monitored by uv-visible spectrometry and GNP were characterized SEM, TEM and AFM analyses.

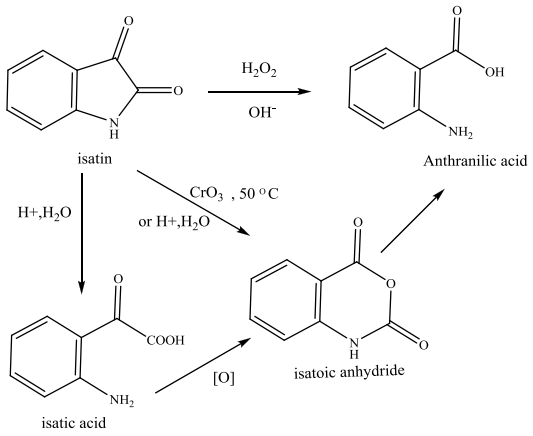

Scheme 2: Oxidation pathways of isatin

Materials and Methods:

1. Chemicals and Instruments:

All the following chemicals in this study were used as received from suppliers: Isatin (1H-(indole-2, 3-dione 99%) was purchased from Aldrich. Sodium tetrachloroaurate (III) trihydrate ($NaAuCl_4.3H_2O$), potassium hydrogen phthalate (2-(HO_2C) $C_6H_4CO_2K$, 99.95%), potassium chloride 99%, and dipottasium hydrogen orthophosphate (K_2HPO_4, (99%)) were purchased from BDH., potassium dihydrogen orthophosphate (KH_2PO4, 99%) and sodium hydroxide (99.95%) were obtained from Fluka AG. The absorption spectra in the uv-visible region 200- 1100 nm were recorded on a SHIMADZUE 1800 Double Beam UV-Vis spectrophotometer. TEM images were acquired using Philips CM10 transmission electron microscope. Samples for TEM studies were prepared by placing a drop of the gold colloidal solution on TEM carbon coated copper grid and was left to dry under vacuum for 48h . SEM images were acquired using TE SCAN VEGA 2, Creech electron microscope. GNPs solutions were applied on slides and dried by vacuum spin coater instrument. AFM images were obtained using AFM model AA 3000

SPM 220 V-Angstrom Advanced Inc. USA. All sample solutions were dialyzed prior to analysis by using a cellulose tube (MW cutoff 12 400 D) against 1 L of DDW for 9 h at 30 °C. Fourier transform infrared spectroscopy (FTIR) spectra within the wavenumber region between 4000 and 200 cm^{-1} were recorded on a SHIMADZUE FT-IR 8400S Fourier transforms spectrophotometer, using KBr and CsI pellets. XRD measurements were performed using a SHIMADZUE XRD-6000 X-ray diffraction spectrometer.

2. Preparation of Solutions

A stock solution of gold salt (5×10^{-3}M) which contains 2.5×10^{-3} M of Au^{3+} ions was prepared by dissolving 0.1000 gm. of sodium tetrachloroaurate trihydrate ($NaAuCl_4.3H_2O$) in 50 ml distilled deionized water (DDW) in 50 ml volumetric flask. Working standard solution of $NaAuCl_4$ (5×10^{-4} M) which contains 2.5×10^{-4} M of Au(III) ions, was prepared by diluting 10 ml of stock solution to 100 ml with DDW. Isatin stock solution (6.8×10^{-3} M) was prepared by dissolving (0.1000 gm) of isatin in 100 ml (DDW) in a 100 ml volumetric flask. Working standard solutions of isatin (6.8×10^{-4} M) were prepared by diluting 10 ml of stock solution to 100 ml with (DDW) in a 100 ml volumetric flask.

3. Optimization of nanoparticle synthesis

3.1. Concentration of isatin

To study the effect of isatin concentration on GNp synthesis, one ml aliquots of gold standard solution were added to ten (5 ml) volumetric flasks containing (0.25 ,0.5 , 0.75 , 1.0, 1.25 , 1.5 , 2.0, 2.5 , 3.0, and 3.5 ml) isatin standard solutions (6.8×10^{-4} M) followed by dilution to 5 ml by DDW. The absorption spectra of all prepared solutions were measured at different time intervals.

3.2. pH of solutions

Synthesis of GNPs was studied at pH : 2.4, 2.89, 3.84, 4.85, 5.80, 6.92, 7.55, 8.92, 9.90, 10.90, and 11.86. Aliquots of 1.5 ml of Au(III) standard solution ($2.5x10^{-4}$) were added to eleven 5ml volumetric flasks containing 1.5 ml isatin standard solution (6.8×10^{-4} M) followed by dilution to 5 ml with the suitable buffer solution. Then absorbance of each solution was measured at different intervals at room temperature.

Results and Discussion:

1. Uv-visible spectrophotometry

The synthesis of GNPs was monitored by uv-visible spectrophotometry. GNPs show a strong absorption band in the visible range due to surface plasmon resonance absorption, the energy of which is dependent on size and shape of the particles [13,29-31]. For roughly spherical GNPs, one single band is observed in the visible region with a maximum falls between λ 520 and 550 nm [6, 7, 11,12, 23, 29-32]. In the present work a primary testing of GNPs synthesis was carried out in aqueous solutions by simple mixing of equal volumes of Au(III) and isatin dilute standard solutions (0.05 and 0.136 mM respectively) with a concentration ratio of [Is] /[Au(III)] = 2.72 without the addition of reducing agent. The uv–visible spectra of isatin, $AuCl_4^-$ and the GNPs solutions in DDW are shown in Figure 1. The spectrum of isatin displayed two high intensity bands at λ 249 and 296 nm and a lower intensity band at 420 nm attributed to $\pi\rightarrow\pi*$ and $n\rightarrow\pi*$ transitions respectively[44]. The $AuCl_4^-$ solution exhibited a high intensity band at λ 240 nm with a shoulder at λ 290 nm assigned to ligand to metal charge transfer transitions (LMCT) of tetrachloroaurate complex [24,25]. The

mixture of both reactants produced a pink red colored solution with an absorption peak observed at λ 538 nm indicating that $AuCl_4^-$ has been reduced by isatin to form GNPs. The spectrum exhibited also a hypsochromic shift of the isatin $n\rightarrow\pi*$ transition band to 400 nm. No additional band was observed in the visible or NIR region which refers to the formation of spherical gold nanoparticles [6,7,11,12, 23, 29-32].

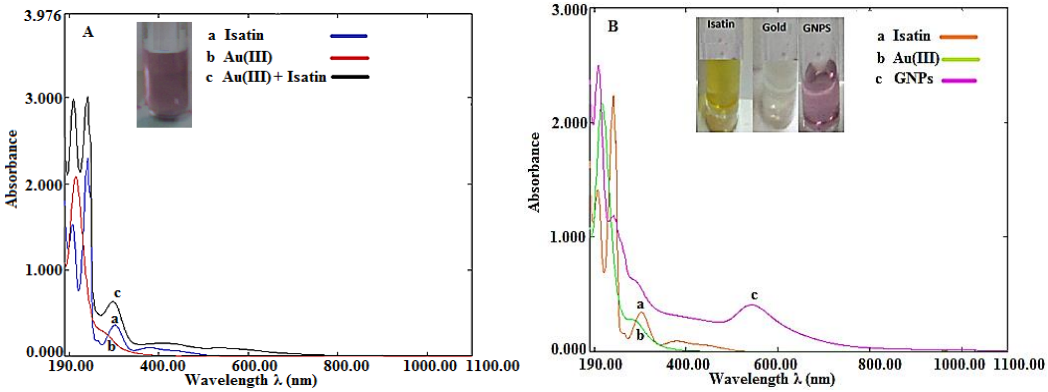

Fig. 1: The uv-visible spectra of a- isatin (0.136 mM) , b- $AuCl_4^-$ (0.05 mM of Au(III) ions) and c-synthesized gold nanoparticle in aqueous solutions at room temperature A- after 1h and B - after 24 h . The images show the pink color of the spherical gold nanoparticles for the two periods respectively.

The suggested mechanism of the reduction process may involves the oxidation of isatin by $AuCl_4^-$ to isatoic anhydride followed by a hydrolysis step in water to give anthranilic acid and CO_2 as final products as is illustrated in scheme 3

2. Optimization of reaction conditions

2.1. Concentration

Figure 2 shows the variation of intensity and position of SPB of gold nanoparticles solutions prepared from adding a fixed adding a fixed volume of Au(III) solution to different volumes of isatin which has been monitored by uv-visible spectrophotometry.

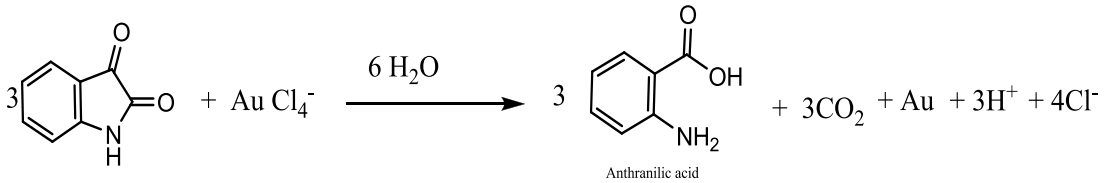

Scheme 3: The suggested mechanism of $AuCl_4^-$ reduction by isatin.

The concentrations of isatin solutions were: 0.034, 0.068, 0.102, 0.136, 0.170, 0.204, 0.272, 0.34, 0.408, and 0.476mM while the Au(III) concentration was kept constant at 0.05mM. The concentration ratios Is/Au(III) of the resulting solutions are: 0.68, 1.36, 2.04, 2.720, 3.4, 4.08, 5.44, 6.9, 8.16, 9.52 respectively). At low isatin concentrations 0.034- 0.136, (samples 1-4) clear pink to purple colored solutions were obtained. After 2h of preparation the spectra of the first three solutions exhibited two bands : a high energy band at λ 532, 535, 533 nm respectively and a low energy band at 750,775- 800 (broad) and 750 nm respectively. After 24 h the high energy bands were shifted to shorter wavelengths

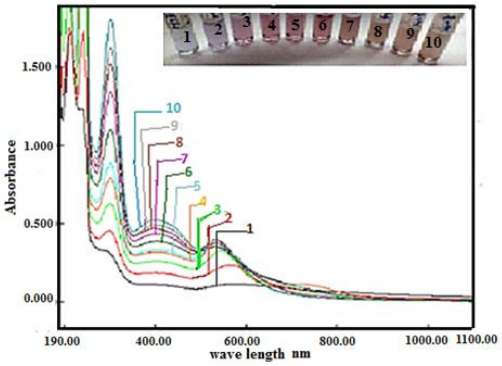

Fig. 2: Absorption spectra of GNP at different concentrations of Is after 24 h.

(λ 531,529,532 nm respectively) while their low energy bands appeared at (889, 788, and 750 respectively). These results are attributed to the formation of elongated GNPs aggregates or gold nanorods [7,10,13,23-25]. The higher energy peak represents the surface plasmon resonance along transverse direction similar to that from nanospheres while the second peak arises from the surface plasmon along the longitudinal direction [26-28]. At higher isatin concentrations (samples 5-10, Is/Au (III) 3.4- 9.52), only one single absorption band was observed at 532-537 nm corresponding to the SP resonance of spherical GNPs with estimated size range of 40-60nm diameter [29-31]. After 24h the position of SPB of these solutions was shifted to shorter wavelength side (528- 532 nm) and the full width at half maximum (FWHM) of the spectrum decreased with increasing Is/Au(III) ratio. The samples were stable for more than 6 weeks. This implies that reduction of Au (III) with different isatin concentrations can determine the size and shape of synthesized GNPs. It also implies that high Is/Au (III) ratio is necessary to achieve high rate of reduction which agrees with results obtained from synthesis of GNPs using other reducing agents [1, 49-51]. The variation of SPR absorption spectra of GNPs solution with time using 0.17 0.476 mM of Is and 0.05M Au(III) solution are shown in Figures 3.

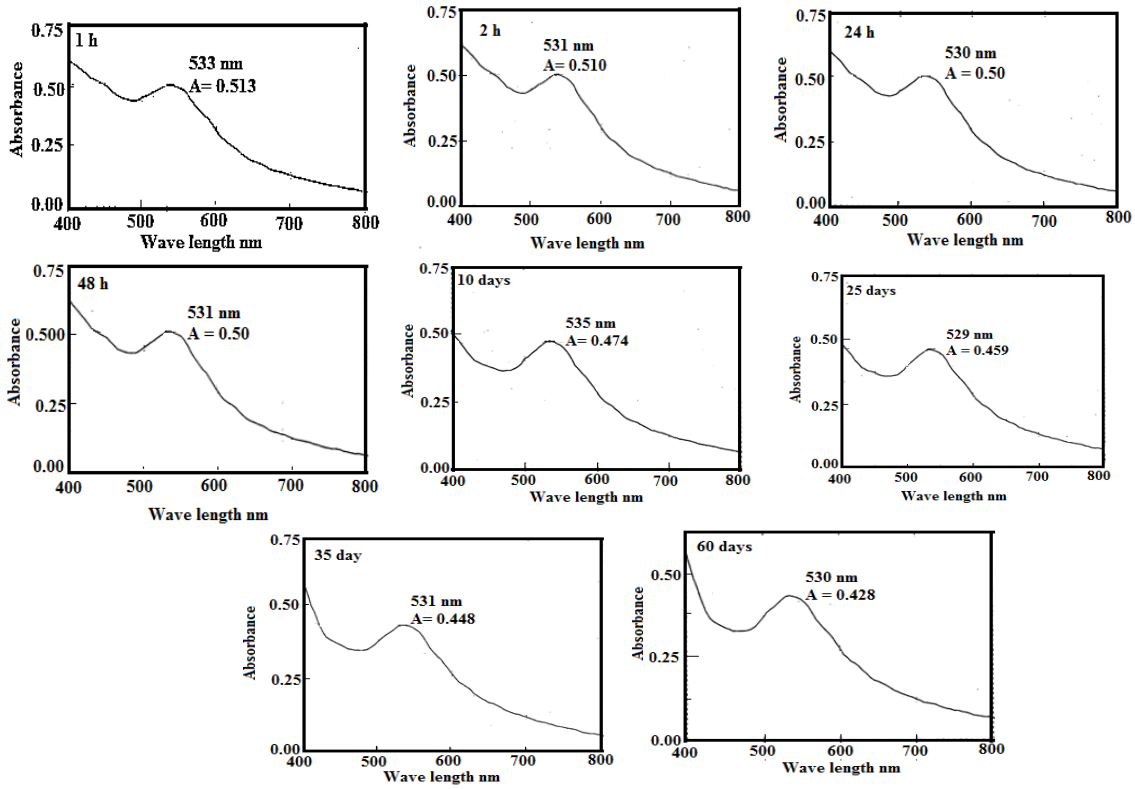

Fig. 3: Variation of SPR with time for GNPs prepared from a solution containing 0.476 mM Is and 0.05 mM Au (III) solution. Concentration ratio of Is/Au (III) = 9.52

2.2. Characterization of prepared GNPs

The size ranges of the gold nanoparticle lie between (32-96) nm [**11**]. Figures 4a and 4b show the images of TEM (transmission electron microscope) and SEM (scanning electron microscope) respectively for gold nanoparticles prepared by mixing equal volumes of isatin and $AuCl_4^-$ standard solutions. In the TEM image the size range of the nanoparticle lie between 23-50 nm and the Au nanoparticles are spherical in shape with smooth surface morphology. The SEM image shows a particle size distribution in the range of 30- 72 nm diameter with spherical surface morphology and the sample displays high dispersion. On the other hand the particle size distribution of AFM image showed that the average particles diameter was around 71.63 nm as is shown in Figure 5.

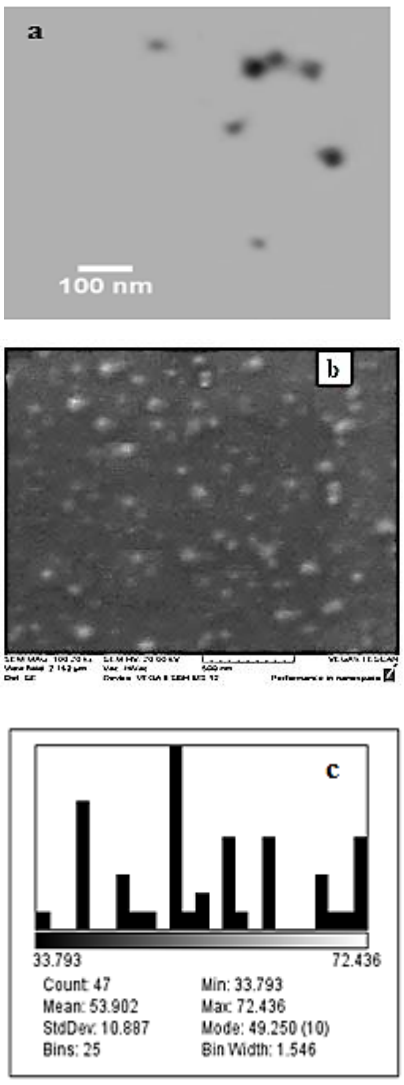

Fig. 4: a- TEM and b- SEM images with c-particle size distribution of the synthesized GNPs

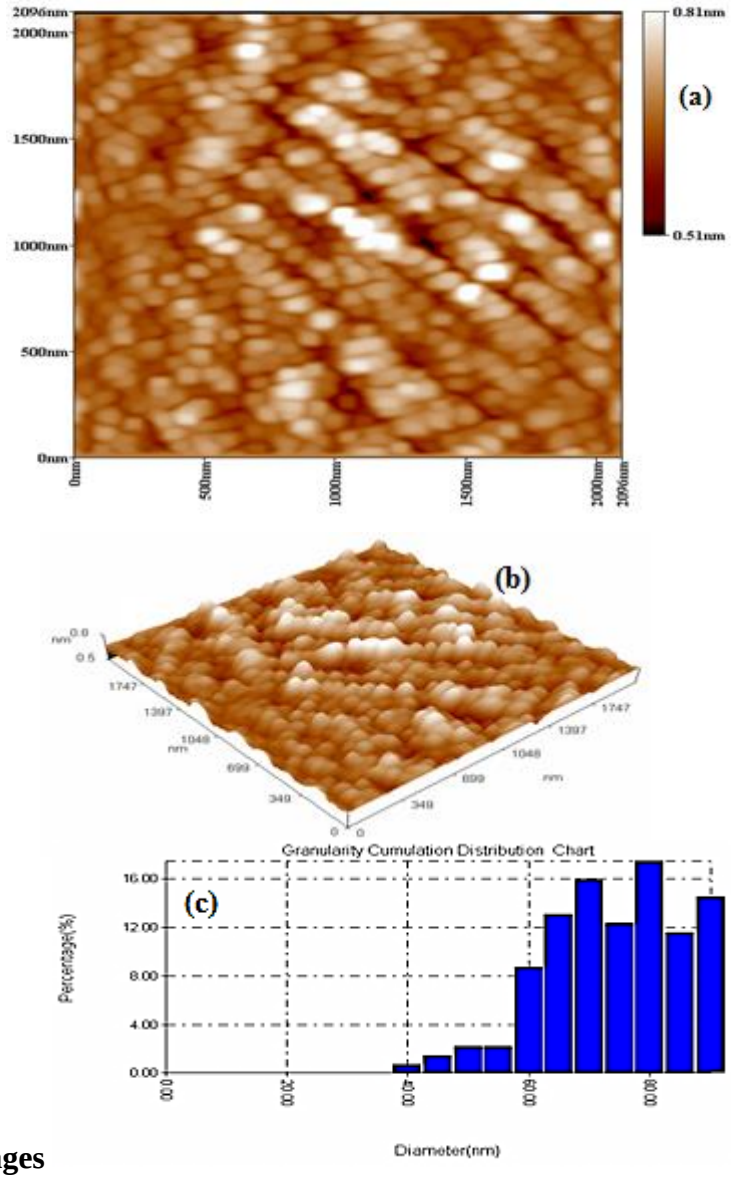

Fig. 5: (a) 2-D and (b) 3-D AFM pictures with granularity cumulation distribution chart (c) of the synthesized GNPs. Average particles diameter 71.63 nm

The size difference in these results may be attributed to the technical sample preparation techniques. The XRD pattern of GNPs (Figure 6a) showed two diffraction peaks at 2θ = 38.1923 and 44.025 degrees corresponding to the planes 111 and 200 of face centred cubic fcc Au metal crystal lattice respectively[11, 26]. The two additional low intensity diffraction peaks at 2θ =32.86 and 27.74 degrees may be closely related to isatin monoclinic crystal structure corresponding to the planes 022 and 122 respectively (Figure 6b). The first peak may also be related to orthorhombic crystal structure of anthranilic acid corresponding to the 400 plane which was observed at 2θ = 27.707 degree (Figure 6c). These results indicate that isatin and its oxidation product may have been adsorbed on the surface of GNp.

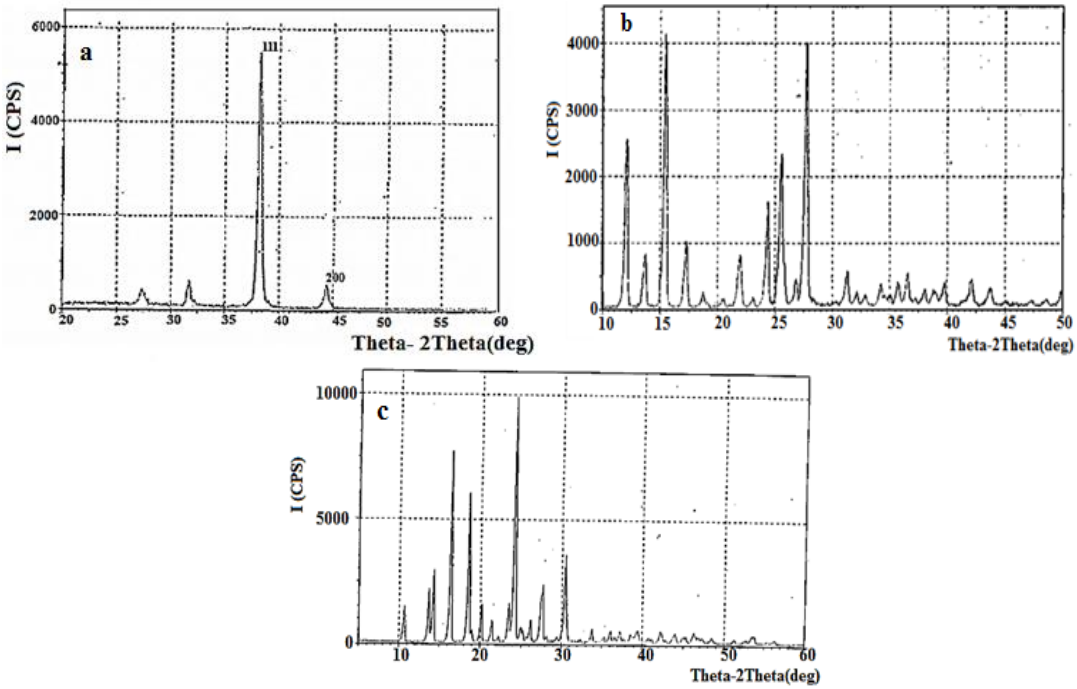

Fig. 6: XRD patterns of a- synthesized GNPs, b- Isatin and c-anthranillic acid

The FTIR spectra of isatin, anthranillic acid and synthesized GNPs are shown in Figures 7a, 7b and 7c respectively. The spectrum of isatin shows two strong bands at 1746 (sh) and 1728 cm^{-1} assigned to the C-3 and C-2 carbonyls and a third strong band at 1615 assigned to aromatic C=C stretching vibrations [33,44,46]. The band observed at 3194 cm^{-1} is attributed to the stretching vibrations of NH group [33,44, 46]. The spectrum of anthranilic acid exhibited bands at 3325 and 3240 cm^{-1}, respectively related to asymmetrical and symmetrical NH_2 stretching vibrations while the band assigned to carboxyl carbonyl group appeared at 1662 cm^{-1} [52] . The spectrum of GNPs exhibited a broadening in the absorption band assigned to N-H stretching mode which was observed at wave number range 3433-3250 cm^{-1} and the disappearance of the bands assigned C-3 carbonyl group of isatin. The two bands appeared at 1665 and 1593cm^{-1} respectively may be assigned to C-2 carbonyl of isatin and carboxyl carbonyl group of anthranilic acid. This gives a supportive evidence on the capping of GNPs by carbonyl and amino groups of both isatin and its oxidation product.

3.3 Effect of pH

The effect of pH on the synthesis of GNPs by isatin has been studied at pH range 2.4- 11.85 with time by uv-visible spectrophotometry and results are shown in Figures 8, 9 and 10 while images of GNPs of different solutions with time are shown in Figure 11.

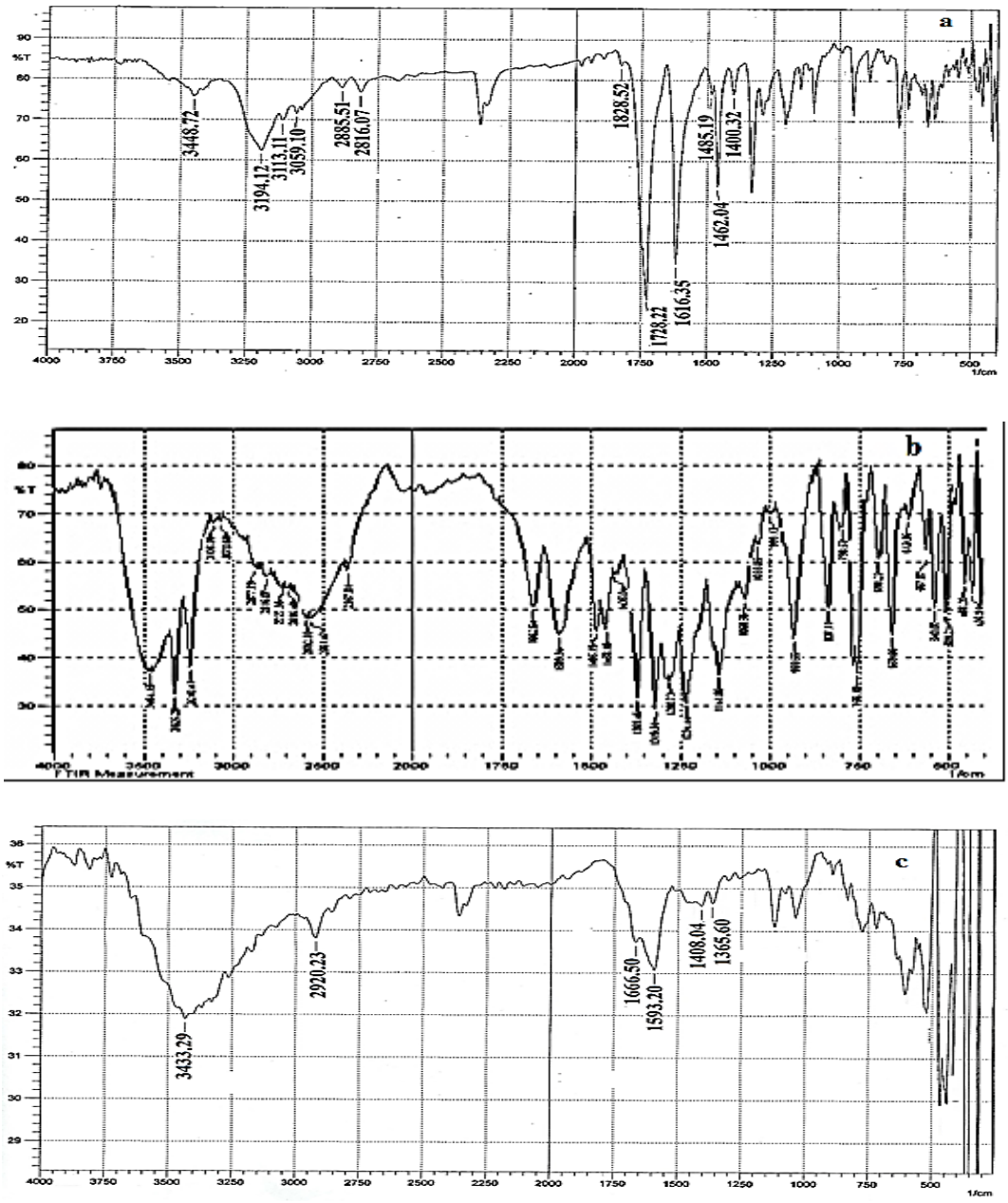

Fig. 7: FTIR spectra of a- isatin, b- anthranilic acid and c- synthesized GNPs

It has been reported that the reduction of $AuCl_4^-$ to form monodispersed GNPs increases at low pH as a result of electrostatic repulsion between protonated reducing ligands adsorbed on the surface of GNPs and decrease with increased pH [1, 49,51].

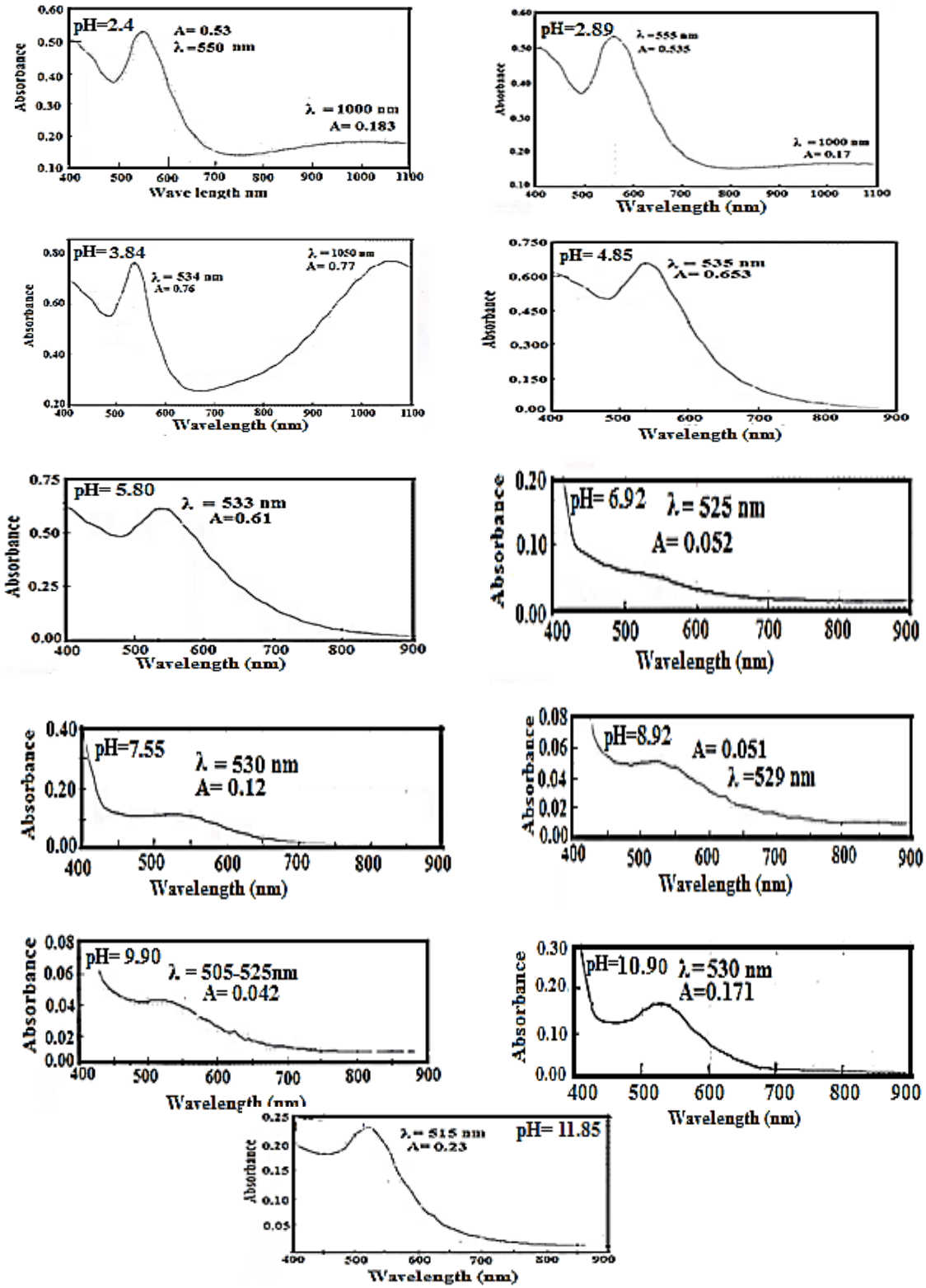

Fig. 8: Absorption spectra of GNP solutions at different pH at room temperature after 24 h.

In this study quite different results have been obtained. After 3h of preparation changes in color and appearance of surface plasmon bands were observed only at pH 4.85 and 5.80 and to less extent at pH 7.55 , 10.90 and 11.85. At pH 6.92, 8.92 and 9.90 no SPBs were observed and

colors of solutions ranged from pale yellow to nearly colorless which refers to incomplete reduction of Au(III) ions. The slow reduction at low pH may be attributed to intermolecular electrostatic attraction between protonated amino group with the deprotonated carboxyl group of the hydrolyzed ligand [21] while the lower reduction rate at pH 7.55 , 10.90 and 11.85 may be attributed to the $Au(OH)xCl_4$-x species which become more stable toward reduction with increased substitution of Cl^- by OH^- ions compared with $AuCl_4^-$ [1, 21]. At pH = 4.85 (purple) and pH 5.80 (violet) solutions exhibited one SPB at λ 527 and 525 nm respectively characteristic of spherical GNPs [6, 7, 11, 12, 23,29-32] with estimated GNP diameter 30-40 nm [29-31] After 24h the position of SPB was shifted with time to 532-536 nm (Figure 9) which refers to larger particle sizes. The GNPs of pH= 4.85 recorded the highest intensity of SPR with time for two weeks. However, after one month the intensity decreased by 60% while at pH 5.80, GNPs colloid was stable for one month without significant changes in colors (Figure 10) and SPB positions (Figures 9). After 24h, solutions of pH = 2.4 and 2.89 showed violet colors and their spectra exhibited sharp bands at λ 550-555 nm and additional low intensity absorption bands covering the near IR range at λ 800-950 nm assigned to longitudinal GNPs [7, 10,13, 26-28,50]. The solution of pH 3.84 was pink red and its spectrum showed also two absorption bands appeared at 527 and 1050 nm. These results show that reduction of $AuCl_4^-$ by isatin at pH range 2.40-3.84, induced the synthesis of elongated GNp (nanorods). After 24h the spectra of of pH 4.85-11.85 GNPs still showed only one single band observed at 528-537 nm corresponding to SPR of spherical GNPs with estimated size range of 40-65 nm [29-31]. At pH 7.55, 10.90 and 11.85 solutions showed pink colors and their spectra exhibited one band only appeared at λ 530-550, 528-530, and 525 nm respectively. After 9 months colloids of pH 6.92 - 11.86, (Figure 13) showed increased extinction and shifts of SPB to shorter wave length (525-532 nm) which refers to the production of spherical GNp with estimated size range of 40-52 nm [6,7,11,12, 23,24,29-31]. On the other hand the solutions of pH 2.4, 2.89 and 4.85 showed sediments and color fading . These results show the effect of pH as an important factor in controlling the reduction potential of isatin as well as the size , shape, stability and rate of formation of GNPs,.

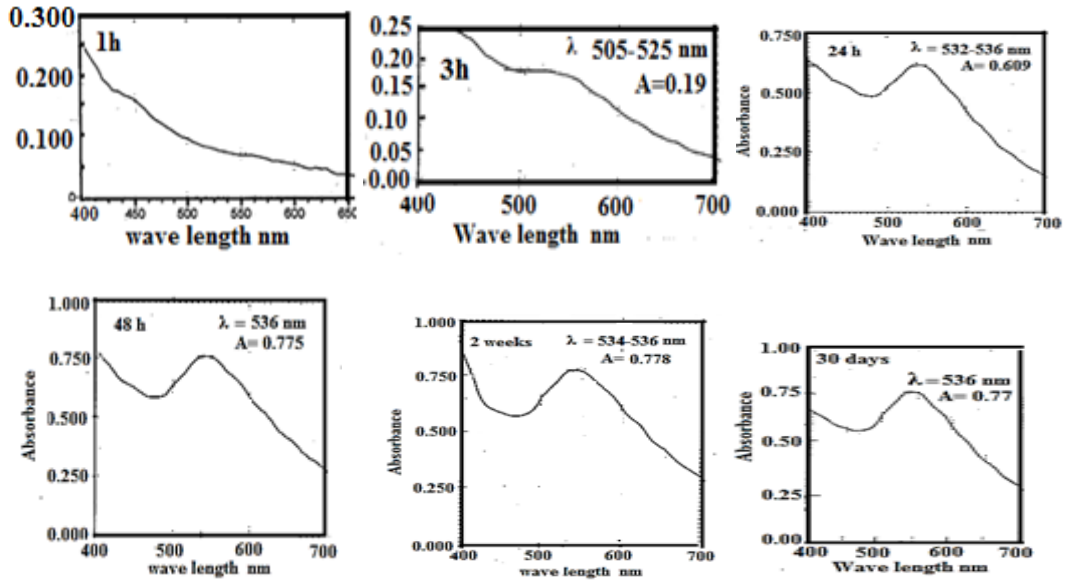

Fig.9 : Variation of SPR of GNPs prepared at pH=5.80 with time

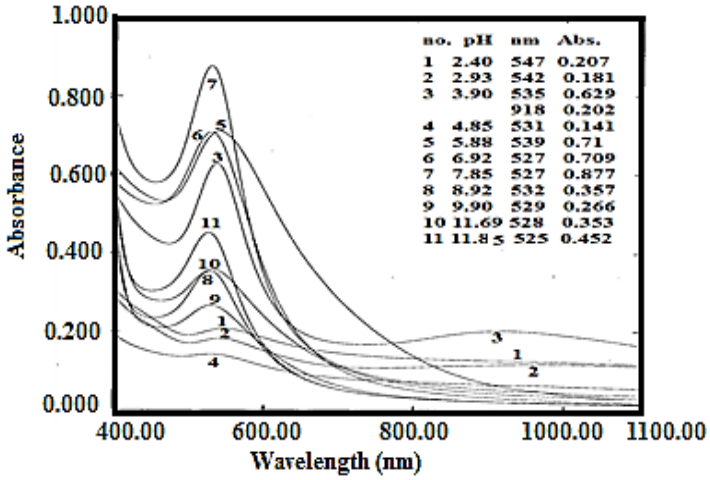

Fig. 10: The spectra of isatin synthesized GNPs at different pH after 9 months

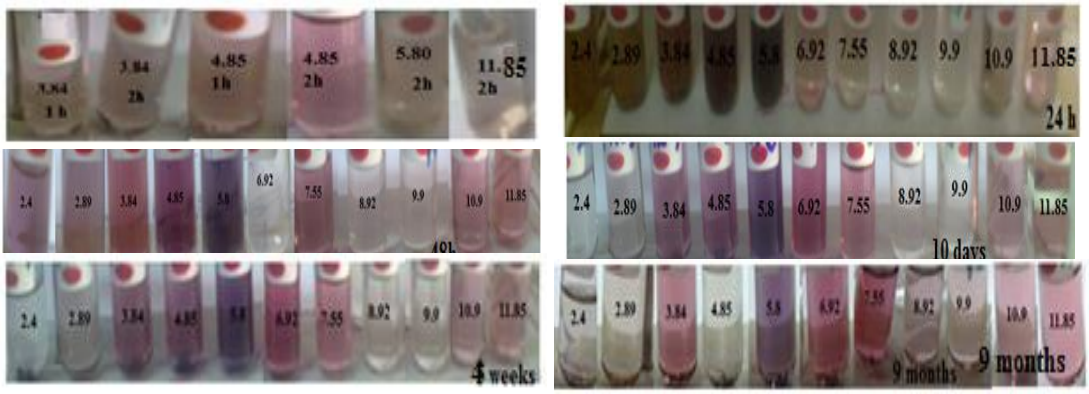

Fig. 11: Color change of the synthesized GNPs solutions with time at different pH

Conclusions:

GNPs with average diameter range 30-72 nm have been synthesized from the reaction of isatin with $NaAuCl_4$ in aqueous solutions at room temperature in the absence of reducing or dispersing agent at different isatin concentrations, different pH and time intervals. Changes in the concentration ratio of Is /Au (III), and pH affect the size, morphology and stability of GNps with time.

Synthesis of spherical GNp at room temperature increased with increased concentration ratio of Is/Au (III) in the range 3.4- 9.52. At concentration ratio 3.4 of Is/Au(III) optimum conditions of GNPs synthesis with SPR absorption at 528-536 were achieved at pH 5.8. Increasing the reaction temperature and the addition of surfactant had a remarkable effect on synthesis rate and sizes of GNPs as will be reported in our future work.

Acknowledgment:

The authors wish to thank Dr. Abdul-Kareem M. Ali for performing the AFM analysis and Miss Muneera K. Ahmed for performing the uv-visible spectral measurements.

References:

1. Young J. K., Lewnski N. L., Langsner R. J., Kennedy L. C., Satyanarayan A., Nammalvar V., Lin A. Y. and Drezek R. A. , 2011. Size- controlled synthesis of monodispersed gold nanoparticles via carbon monoxide reduction, *Nanoscale Res. Lett.*, 6: (428): 1-11.

2. Eustis, S. and Elsayed, M. A., 2006. Why gold nanoparticles are more precious than pretty gold: noble metal surface plasmon resonance and its enhancement of the radiative and nonradiative properties of nanocrystals of different shapes. *Chem. Soc. Reviews*, 35, 209-217.

3. Olejnk, M. Bujak, L. and Mckowski, S., 2012. Plasmonic molecular nanohybrids- Spectral dependence of fluorescence quenching, *Int. J. Mol. Sci*., 13: 108-1028.

4. Lee K. Y. , Hwang J., Lee Y. W., Kim J., Han, S.W., 2007. One-step synthesis of gold nanoparticles using azcryptand and their applications in SERS and catalysis, *J. Colloid Interface Sci.*, 316, 476-481.

5. Sobczac-Kupiec A., Malina D., Zimwska M. and Wzorek Z., 2011. Characterization of gold nanoparticles for various medical applications, *Dig. J. Nanomater Bios.*, 6(2): 803-808.

6. Bhumakar D. R., Joshi, H. M., Sastry M. and Pokharkar V. B., 2007. Chitosan reduced gold nanoparticles as novel carriers for transmucosal delivery of insulin, *Pharmaceut. Res.*, 24(8): 1415-1426.

7. Boopathi S , Senthilkumar S. , and Phani K. L., 2012. Facile and one pot synthesis of gold nanoparticles using tetraphenylborate and polyvinyl pyrrolidone for selective colorimetric detection of mercury ions in aqueous medium, *J. Anal. Methods Chem.*, 2012, Article ID 348965: 1-6 .

8. Chen P. C., Mwakwari S, C. and Oyelere A. K., 2008. Gold nanoparticles: From nanomedicine to nanosensing, *Nanotechnol. Sci. Appl.*, 1, 45–66.

9. Saha, B., Bhattacharya, J., Mukherjee, A., Ghosh A. K., Santra C. R., Dasgupta A. K. and Karmakar, P.I., 2007. In vitro structural and functional evaluation of gold nanoparticles conjugated antibiotics, *Nanoscale Res. Lett*., 2, 614–622.

10. Wang, W., Chen, Q., Jiang C., Yang D., Liu X. and Xu S., 2007.

One- step synthesis of biocompatible gold nanoparticles using gallic acid in the presence of poly-(N-vinyl-2-pyrroldone), *Colloid and Surfaces A: Physico. Chem. Eng. Aspects***,** 301, 73-79.

11. Das R., Nath S. S. and Bhattacharjee R., 2011. Optical properties of linoleic acid protected gold nanoparticles, *J. Nanomater.***,** 2011, article ID 630834, 1- 4.

12. Ghosh D., Sarkar D., Girigoswami A. and Chattopadhyay N., 2011. A fully standardized method of synthesis of gold nanoparticles of desired dimensions in the range 15-60 nm, *J. Nanosc. Nanotechnol.*, 11,1141-1146.

13. Singh P. P. and Bhakat C., 2012. Synthesis and characterization of colloidal gold nanoparticles suspension using liquid soap, *Chem. Mater. Res.*, 2 (1): 82-87**.**

14. Tu M. H., Sun T. and Grattan K.T.V., 2012. Optimization of gold-nanoparticle-based optical fibre surface plasmon resonance (SPR)-based sensors, *Sens. Actuators B Chem.***,** 164, 43– 53.

15. Singh C., Sharma V., Krnaik P., Khandelwal V. and Singh H., 2011. A green biogenic approach for synthesis of gold and silver nanoparticles using *Zingiber officinale, Dig. J. Nanomat.. Bios.*, 6(2): 535-542.

16. Newman J. D. S. and Blanchard G. J., 2006. Formation of gold nanoparticles using amine reducing agents, *Langmuir,* 22, 5882-5887.

17. Subramaniam C., Tom R. T. and Pradeep T., 2005. On the formation of protected gold nanoparticles from $AuCl_4^-$ by the reduction using aromatic amines, *J. Nanopart. Res.*, 7,209–217.

18. Warsi M. F., Afzal M. A., Mahmood A., Javed S., Qureshi A.M. and Shahid M., 2012.Short tail tryptophan-functionalized gold nanoparticles: synthesis, characterization and their fluorescent quenching behavior. *New Horizons Sci. Technol. (NHS&T),* 1(2): 33-35.

19. Akbarzadeh A., Zare D., Farhangi A., Mehrabi M. R., Norouzian D., Tangastaninejad S., Moghdam M. and Bararpour N.**,** 2009. Synthesis and characterization of gold nanoparticles by tryptophane, *Am. J. App. Sci.*, 6(4): 691-695.

20. Mandal S., Selvakannan P., Phadtare S., Pasricha R. and Sastry M.**,** 2002**.** Synthesis of a stable gold hydrosol by the reduction of chloroaurate ions by the amino acid, aspartic acid**.,** *Proc. Indian Acad. Sci. (Chem. Sci.),* 114(5): 513–520.

21. Majziki A., Fulop L., Scapo E., Bogar F., Martinek T., Penke B., Biro G. and Dekany I., 2010. Functionalization of gold nanoparticles with amino acid. β-amyloid peptides and fragments, *Colloids Surf., B.: Biointerfaces,* 81, 235-241.

22. Ding Y., Zhang X., Liu X. and Guob R., 2006. Studies on interactions of thionine with gold nanoparticles, *Colloids Surf., A: Physicochem. Eng. Aspects***.** 290, 82–88.

23. Johan M. R., Chong L. C., Hamizi N. A., 2012. Preparation and stabilization of monodisperse colloidal gold by reduction with monosodium glutamate and poly(methylmethacrylate)., *Int. j. Electrochm. Sci.* 7, 4567-4573.

24. Link S. and El-Sayed M. A., 1999. Size and temperature dependence of the plasmon absorption of colloidal gold nanoparticles, *J. Phs. Chem. B,* 103, 4212-4217.

25. Jiang G., Wang L. and Chen W., 2007 Studies on the preparation and characterization of gold nanoparticles protected by

dendrons, *Materials Letters***,** 61, 278-283.

26. Long N. N., Vu L. V., Kiem C. D., Doanh S. C., Nguyet C. T., Hang P. T., Thien N. D. and Quynh L., 2009, Synthesis and optical properties of gold nanoparticles. APCTP-ASEAN workshop on advanced materials science and nanotechnology (AMSN08), *J. Phys.: Conf. Ser.*187, 012026, 1- 8.

27. Shi W., Casas J., Venkataramasubramani M. and Tang L., 2012. Synthesis and characterization of gold nanoparticles with plasmon absorbance wavelength tunable from visible to near infrared region, *Int. Scholarly Res. Net. ISRN Nanomat.*, 2012, Article ID 659043, 1-9.

28. Samal, A. K. and Sreeprasad T. S., 2010. Investigation of the role of $NaBH_4$ in the chemical synthesis of gold nanorods, *J. Nanop. Res.*, 12, 1777-1786.

29. Slouf M., Kuzel R. and Matej Z., 2006. Preparation and characterization of isomeric gold nanoparticles with pre-calculated size, *Z. Kristallogr. Suppl.* , 23, 319- 324.

30. Martínez J. C., Chequer N. A., González J. L. and Cordova T., 2012. Alternative. methodology for gold nanoparticles diameter characterization using PCA technique and uv-visible spectrophotometry, *Nanosci. and Nanotechnol.*., 2(6):184-189.

31. Jain L. and El-Sayed M., 2006. Calculated absorption and scattering properties of gold nanoparticles of different size, shape, and composition: applications in biological imaging and biomedicine, *J. Phys. Chem. B*, 110, 7238-7248.

32. Xavier B., Ramanand A. and Sagayaraj P., 2012. Investigation on a facile one-pot rapid synthesis approach for developing modestly monodispersed and stable spherical gold nanoparticles, *Der Pharm. Chem.*, 4(4): 1467-1470.

33. da Silva J. F. M., Garden S. J. and Pinto A. C., 2001. The chemistry of isatins: a review from 1975 to 1999. *J. Braz. Chem. Soc.*, 12(3):273-324.

34. Raj V., 2012, Review on CNS activity of isatin derivatives, *Int. J. of Curr. Pharmaceut. Res*. 4(4): 1-9.

35. Pal M., Sharma N. K. and Jha P. K., 2011. Synthetic and biological multiplicity of isatin: a review, *J. Adv. Sci. Res.***,** 2(2): 35-44.

36. Vijayabaskaran M., Lakshmi G., Senthilraja M., Sivakumar P. and Perumal P., 2011. Synthesis and antimicrobial studies of some novel isatin derivatives, *J. Pharm. Res.*, 4(10): 3664-3666.

37. Bhrigua] B., Pathaka D., Siddiqui N., Alam M. S. and Ahsan W., 2010. Search for biologically active isatins: a short review, *Int. J. Pharmaceut. Sci. Drug Res.*, 2(4): 229-235.

38. Cândido-Bacania P. de M., Reisa M. B. dos, Serpelonia J. M., Calvo T. R., Vilegas W., Varandac E. A. and Cólusa I. M. de S., 2011. Mutagenicity and nontoxicity of isatin in mammalian cells in vivo**,** *Mut. Res.***,** 719, 47–51.

39. Hoque M. and Islam R., 2008. Cytotoxicity study of some indophenines and isatin derivatives," *Bangladesh J. Pharmacol***.** 3, 21-26.

40. Zaranappa, Chaluvaraju K. C., 2011. Synthesis and biological evaluation of some isatin derivatives for antimicrobial properties, *Res. J. Pharmaceut. Biol. Chem. Sci.***,** 2(1): 542- 546.

41. Mana S., Pahari N. and Sharma N. K., 2010. Synthesis and characterization of novel thiazolo-isoxazole fused isatin as analgesic

and anti-inflammatory agent, *T. Pharm. Res.*, 3, 51-59.

42. Sonawane A. E., Pawar Y. A., Nagle P. S. and More D. H., 2009. Synthesis of 1,4-benzothiazine compounds containing isatin hydrazine moiety as antimicrobial agents**,** *Chin. J. Chem.***,** 27, 2049 - 2054.

43. NagarajanG., Balasubramaniam V., Manjunath K.S., Ramakrishna E., Reddy K. P. K., Reddy E. K. and Girija K., 2008. Synthesis and *in vitro* cytotoxic activity of isatin derivatives, *Asian J. Chem.*, 20(3): 1665-1669.

44. Khalil M. M. H., and Al-Seif, F. A., 2008, Molybdenum and tungsten tricarbonyl complexes of isatin with triphenylphosphine, *Res. Lett. Inorg. Chem.*, 2008, Article ID 746058, 1-4.

45. Aliyu H. N. and Suleiman Z., 2012. Spectrophotometric analysis on anticonvulsant bis (N-isatin benzene-1-hydroxy-2-iminato) Mn(II), Fe(II) and Co(II) complexes, *Global Adv. Res. J. Microbiol.*, 1(5): 079-083.

46. Pârnãu, C., Kriza A., Popa N. and Udrea S., 2005. Controlled synthesis III. Reaction Sn(IV) and Zr(IV) with isatins, *Analele Universităţii Bucuresti – Chimie, Anul XIV***,** I-II, 141-146.

47. Kappe P. and Staddlebaur W., 1981. Isatoic anhydrides and their uses in heterocyclic synthesis, *.Adv. heteroc. Chem.*, 28, 127-178.

48. Deligeorgiev T., Vasilev A., Vaquero J. J. and Builla, J. A., 2007. A green synthesis of isatoic anhydrides from isatins with urea–hydrogen peroxide complex and ultrasound, *Ultras. Sonochem.*, 14, 497–501**.**

49. Li C., Wan D., Xu J. and Hou W., 2011. Facile synthesis of gold nanoparticles with low size distribution in water: temperature and pH controls, *Nanoscale. Res. Lett.*, 6 (440): 1-10.

50. Morrow, B. J., Matijevic E. and Joia D. V., 2009. Preparation and stabilization of monodispersed colloidal gold by reduction with amino dextran, *J. Coll. Interf. Sci.*, 335, 62-69.

51. Zhang T., Wu Y., Pan X., Zheng Z. , Ding X. and Peng Y., 2009. An approach for the surface functionalized gold nanoparticles with pH responsive polymer by combination of RAFT and click chemistry, *Eur. Polym. J.*, 45, 1625-1633.

52. Kamnev A. A., Kusman E., Prfiliev Y. D., Vanko G. and Vertes A., 1999. Mössbaur and FTIR spectroscopic studies of iron anthranilates coordination, structure and some ecological aspects of iron complexation, *J. Molec. Str.*, 482 - 483, 703-711.

تحضير دقائق الذهب النانوية بالاختزال الكيميائي لايونات الذهب (3+) بواسطة الازاتين في المحاليل المائية: تاثيرات تراكيز الليكاند والدالة الحامضية

*احلام جميل عبد الغني** *رشا خضر حسين**

*جامعة بغداد، كلية العلوم، قسم الكيمياء، الجادرية، بغداد، العراق

الخلاصة:

تم تحضيردقائق الذهب النانوية من اختزال انيونات رباعي كلورو الذهب (3+) ($[AuCl_4]^-$) بواسطة الازاتين (1-H-اندول-3,2 – داي- اون) في المحاليل المائية بدون اضافة العوامل المختزلة والمشتات. تم تشخيص الدقائق النانوية باعتماد قياسات مطيافية الاشعة فوق البنفسحية-المرئية وتحاليل المجهر الالكتروني الماسح (SEM, TEM) ومجهر القوى الذرية (AFM) وحيود الاشعة السينية (XRD) وتحاليل مطيافية FTIR . تمت متابعة عملية الاختزال باعتماد قياسات اطياف امتصاص الاشعة فوق البنفسحية-المرئية للمحاليل النانوية مع تغير الوقت وتركيز الليكاند والدالة الحامضية للمحاليل . كانت تراكيز الازاتين المستخدمة تقع في المدى 0.034-0.476 مللي مولاري. وجد بان سرعة الاختزال لتكوين محاليل نانوية مستقرة تمتلك قمة امتصاص رنين سطح البلازمون (SPB) ذات شدة عالية في المدى الموجي λ 535-530 نانومتر تزداد بزيادة تراكيز الازاتين في المدى 0.170 - 4.76 مللي مولاري. تمت ايضا دراسة تاثير الدالة الحامضية (pH) طيفيا على سرعة تحضيرواستقرارية وشكل وحجم الدقائق النانوية. افضل النتائج كانت عند الدالة الحامضية 5.8 .